Application of Cone beam CT Isocenter Adjustments in Image Reconstruction

Nnadozie M. Ezerioha[1, 2], Thomas Kroc, PhD[1]

[1]Fermi National Accelerator Laboratory (FNAL) Batavia, Illinois, 60510. U.S.A.

[2]Benedict College, Columbia, SC. 29204.

Abstract

The Cone Beam Computed Tomography (CBCT) System at Fermilab is being developed to accurately locate tumors and characterize the surrounding anatomy prior to Neutron Therapy (NT). The aim of this project is to aid accurate prediction of the position of the CT isocenter. This is necessary to ensure spatial isotropy in the reconstructed CT images.The benefits of a cone beam CT include reduction in the total scan time as well as the amount of radiation dosage affecting normal tissue located around cancerous cells. Developed reconstruction algorithms need to be precise to about one degree of rotation.The cone beam CT now being developed will be used alongside the vertical CT to characterize the tumor volume prior to irradiation. At Fermilab, the neutron therapy facility is constructed around a linear accelerator (LINAC), hence the beam is applied in a fixed horizontal position on a lower level while the patient is sitting or standing on a rotating platform. With the location of the beryllium target and collimators well below ground level, an elevator is required to move the patient down from the upper CT level for treatment at the lower NT level after the initial CT scan. The elevator has been determined to have a pitch in the x-y plane (upstream of the beam and transverse to the movement of the elevator). This results in a pixel offset in the reconstructed image. This paper covers the various methods and experiments aimed at measuring the offsets as well as their application in the image reconstruction algorithm.

Key words: isocenter, cone beam CT, alignment, offsets

Introduction

The Neutron Therapy Facility at Fermilab is built to utilize protons deflected from the linear accelerator (LINAC). The neutron beam used to treat malignant tumors is formed by bombarding a beryllium target with these protons which carry 66 MeV of energy. Carefully built collimators are used for focusing the neutron beam which is then used to irradiate the patient's tumor. Neutrons possess a high Linear Energy Transfer (LET). Certain cancerous cells and tumors may exhibit hypoxia which allows the cell's repair mechanism to function better and resist radiation [1]. The reason for this effect is that oxygen reacts chemically with the fundamental biological lesions produced by ionizing radiation. Oxygen possesses the highest electron affinity in the cell and thus reacts extremely rapidly with the free electron of the free radical; making the damage permanent. Therefore the oxygen effect can be said to increase the sensitivity of normal tissue to radiation [8]. In the absence of oxygen, much of the radical damage can be restored to its undamaged form by hydrogen within the cells [2]. High LET has been proven effective at treating such resilient cells, hence making neutron therapy a favorable technique [1]. Various studies have also solidified neutron therapy's stance as the best modality for the treatment of a number of resilient human-specific cancers [4] & [9]. Continuing treatment programs will improve the statistical evaluation of these well-established procedures as well as continuing investigation of the treatment of other tumors including bone sarcomas, bladder cancers, carcinomas of the lung, and glioblastoma multiforme. Because neutron beams are so damaging, the risk of side effects on healthy tissue near the cancer site is greater. The neutron beams also diffuse more making its effect on surrounding tissue more profound [7]. For this reason neutron therapy requires very accurate treatment planning mechanisms designed to accurately predict the exact size and location of the tumor.

Materials and Methods

The facility at Fermilab utilizes a continuous, fixed horizontal beam (see Fig. 6) and this requires CT simulation systems that replicate the treatment geometry while performing the simulations. Conventional photon facilities (where the treatment head can be rotated in a circle of approximately 100cm radius about a supine patient) utilize CT simulation whose X-ray components are positioned so that they can acquire the information needed for treatment planning in the exact geometrical relationship as will be used for treatment. Fermilab's horizontal CBCT system is modelled after this. It will increase the accuracy of our existing vertical CT based treatment plans [10] and rule out errors associated with differences in orientation as well as positioning of the patient.

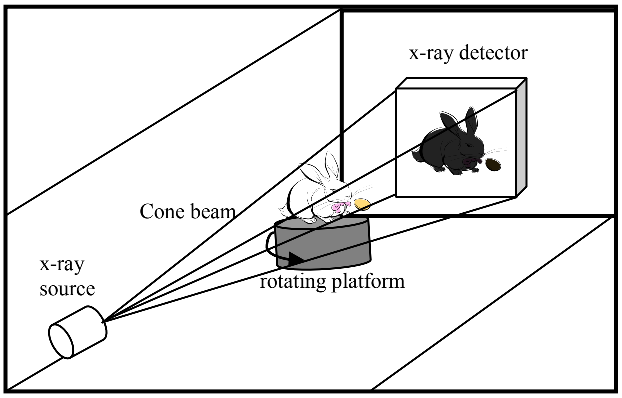

Fig.1. Principle of Cone Beam CT

In conventional CT systems, the electron beam that generates the treatment photons is carried by a "gantry" that can fit in a treatment room that is not much larger than "normal" room dimensions. However because we use protons which are thousands of times more massive than electrons and hence possess a greater kinetic energy, we cannot utilize gantries. If gantries were utilized, they would have to be very massive to contain the protons. This is the reasoning behind employing fixed horizontal beams.

The cone-beam CT system analyzed in this study utilizes a fixed x-ray source and fixed x-ray detector oriented in a horizontal plane and developed by NTF personnel. The CT system in conjunction with the same rotating platform for neutron therapy will be used to provide CT images while in the treatment position. This will mimick the conventional setup used in the less rigid, joint CT simulation/photon treatment systems mentioned earlier.

Our system utilizes an elevator which moves between the top position and a much lower position for neutron irradiation. However, the elevator does not have a perfectly linear trajectory and following tests, continued to present a problem to the anatomical accuracy of the images.

The images produced appeared to have a swirl when the reconstruction algorithm was applied. The practical solution involved measurement of the elevator pitch and applying the offset values calculated. This value was applied to the pixel representing the isocenter in each reconstructed slice of the image. For our studies, a phantom developed by M.A[a] was utilized. Software provided by Exxim [3], was used to locate the position of the fiducial-beads on the phantom.

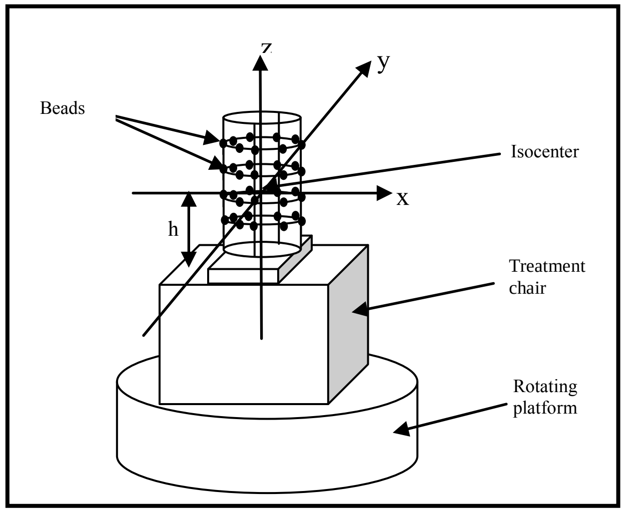

Fig.2. CT Phantom showing height (h) of isocenter from rotating treatment chair

Following survey of the NTF, the following values were obtained as the actual physical offsets in the x, y axes:

Position	Elevator travel	Elevator travel	Elevator travel
Axis	X	Y	Z
Middle	-0.162	-0.256	0.392
Top	-0.108	-0.136	51.448
ΔY, towards downstream	N/A	0.120	N/A
ΔX, towards beam right	0.054	N/A	N/A
ΔZ, towards zenith	N/A	N/A	51.056

Table 1: Offsets in x and y axis.

[a]Mark Austin. biomedical engineer at NIU Neutron Therapy Facility at Fermilab.

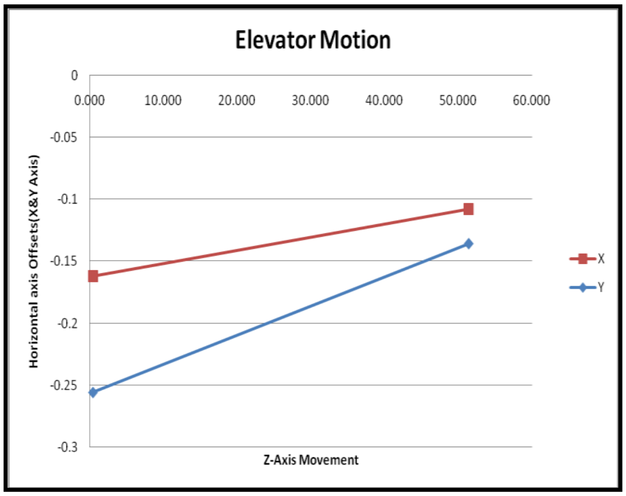

Fig.3. Graph showing motion of elevator with respect to the z-axis

To measure the x and y offsets with respect to the position of the elevator in the z-axis, we installed a position encoder to record the movement of the elevator. A pre-calibrated encoder from Unimeasure Inc., with a range of 200 inches (approx 5m) was acquired (Fig 4). Its options included a side wire rope exit for the length measurements and reversed voltage output.

The voltage output corresponding to the vertical displacement of the elevator was then converted into length and the corresponding transverse offsets in the x and y planes were calculated.

The encoder was then connected to the elevator control module. Pins B and C were connected together internally at the transducer hence C was used as the ground. The device was recalibrated by adjusting the zero and span controls to set zero output voltage and maximum output voltage. The model allows the zero position to be within 0%-30% of range and the maximum position within 80% to 100% [11].

The encoder was installed beneath the elevator and the wire rope attached to the bottom of the elevator. The zero and span adjustments were made to correspond to 4.810V (+/- 0.096) for minimum extension and 0.10V (+/- 0.096) for maximum extension.

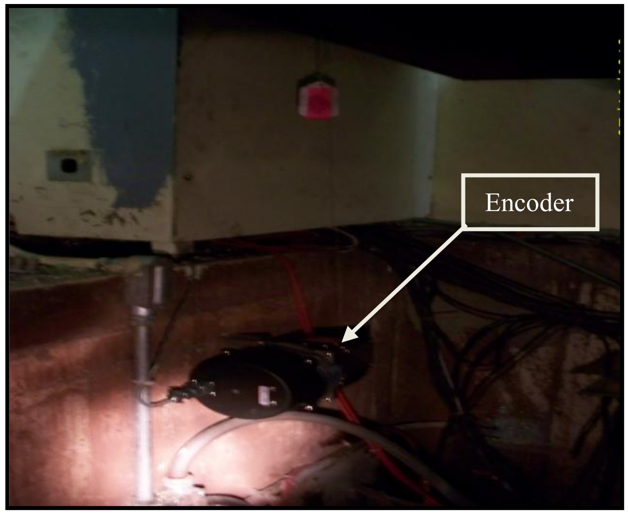

Fig.4. Image of Encoder Installed underneath the elevator

Circuit Design

An Analog to Digital Converter (ADC) was incorporated into a circuit and utilized to convert the analog voltage into binary values. Below is a schematic of the designed circuit.

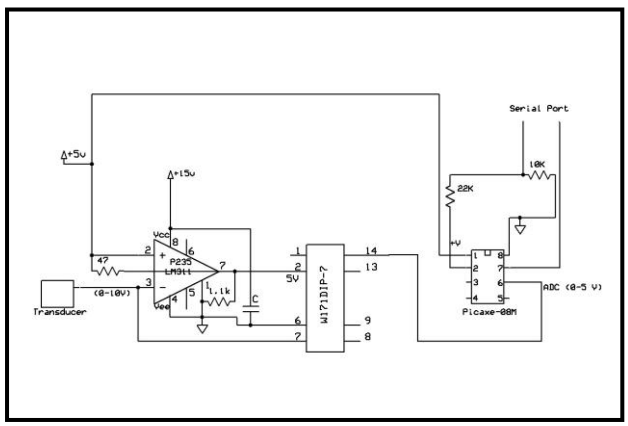

Fig.5. ADC circuit

The preliminary circuit required various adjustments including a shut-off mechanism to stop voltage supply into the circuit once the voltage from the encoder exceeded 5V. This was decided based on the fact that our ADC had a max input voltage of 5V. A comparator was used for this function. The digital data was then read using a C program which reconverts the binary values into voltage and then calculates the

[b] (+/- 0.096)V corresponds to maximum std. dev. shown by ADC in conversion of analog output from encoder. Encoder showed a max *count* deviation of 20 corresponding to 0.096V.

corresponding offset values utilized by the reconstruction program.

Image Acquisition

CT Scans were taken using the CPI Indico 100 X-ray Generator with the following Parameters:

- Horizontal Scan mode
- 55KV
- 2mAS
- Small focal
- Stepsize = 0.5625 degrees
- Number of projections = 361
- Scan from 0 to 202.5 degrees.

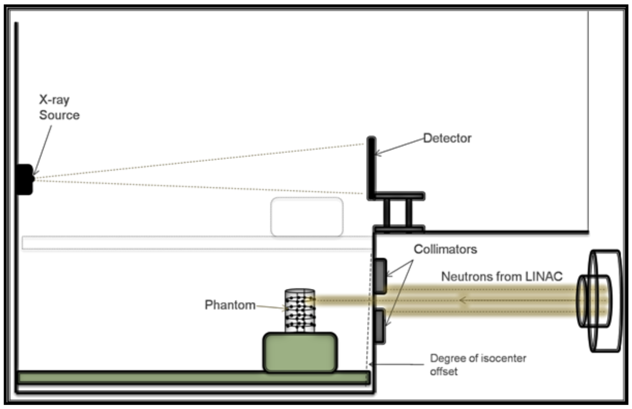

Fig.6. Neutron Therapy Facility (NTF) treatment room

Calibrating Height Measurements

Various scans were taken at different heights (h) to help assess the impact of the movement on the images. Geocalibration software provided by Exxim [3] was then used at this point to detect the positions of the fiducials/beads on the phantom. The software outputs a file containing several parameters which are utilized in the reconstruction of the images.

We recorded data from the position encoder (count and voltage) and from image acquisition software (pivot, U and V). Based on the initial values from the min to max positions, a linear change was observed in the detector pivot parameter. The correction was applied to the template file created by the geocalibration software. This was applied directly in the code. The U and V offsets are determined using the geometrical values calculated which correspond to the shift of the elevator in the x-y plane. The code recreates the calibration file containing the detector pivot, U, and V offsets required for accurate reconstruction.

Results and Discussion

At various elevator levels the following parameters were recorded: *Max voltage: 4.93V, Max count: 1024*

Level	Height (h)	Count	Voltage (v)
Up (Maximum Level)	16.4cm	120	0.570
Middle	44.65cm	430	2.072
Down (MinimumLevel)	89.3cm	958	4.610

Table 2: Elevator level with corresponding count and voltage values

Level	Pivot	U	V
Up (Maximum Level)	-0.386 (100%)	2.373	-29.413
Scan1	-0.193 (36.99%)	2.200	17.442
Down (MinimumLevel)	0.000 (0%)	2.162	62.526

Table 3: Elevator level with corresponding offset values from geocalibration software

Scan 1 respresents a scan taken at a height of 44.65 cm. The height was measured from the top of the rotating platform to the CT isocenter. The percentage count value from our encoder (36.99% here) represents the position of the elevator in space during the scan. This value appeared to be similar to the percentage of height measured from the total height (38.75%) in inches. This showed a difference of 1.76 in our percentage values and thus acceptable accuracy. Further scans showed a similar trend signifying high precision.

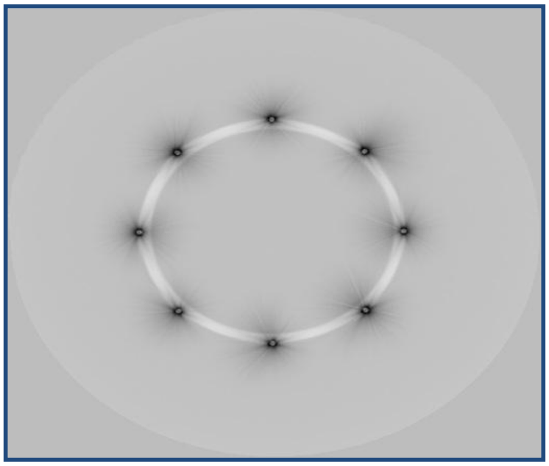

Fig.7a Slice 32
Phantom at h_1= 16.4cm from chair

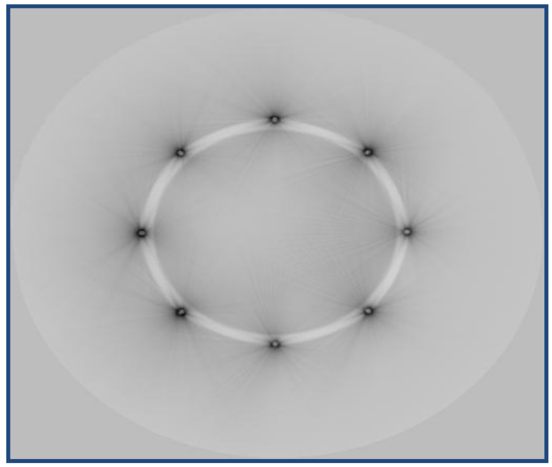

Fig.7b Slice 64
Phantom at h_1= 16.4cm from chair

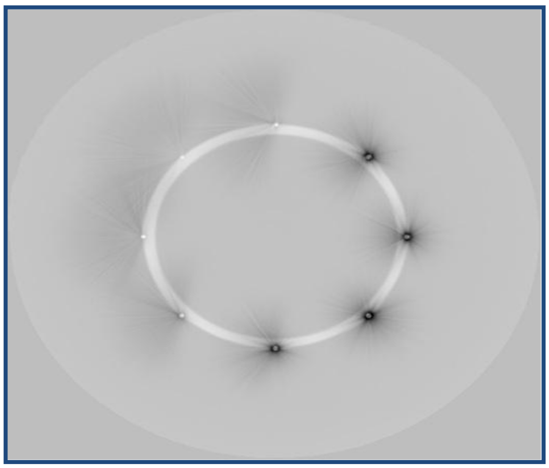

Fig.8a. Phantom down 89.3cm from chair
before correction: Slice 32

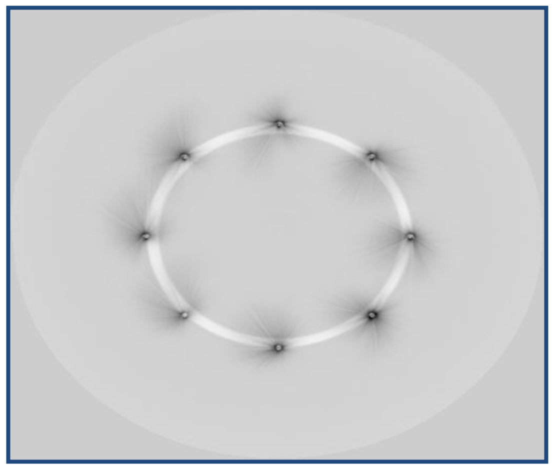

Fig.8b. Down 89.3cm from chair **after** correction: Slice 32

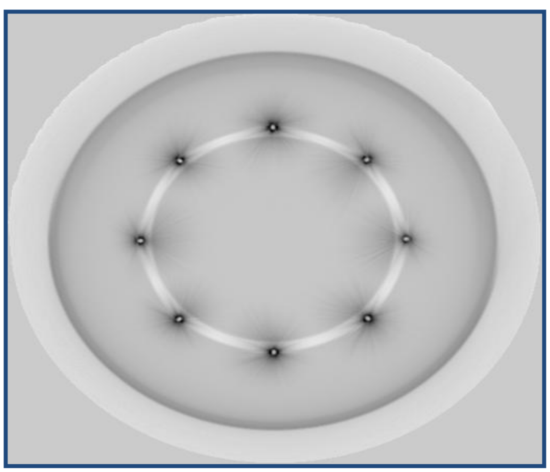

Fig.9a. Phantom down 36.9% from chair
after correction: Slice 32

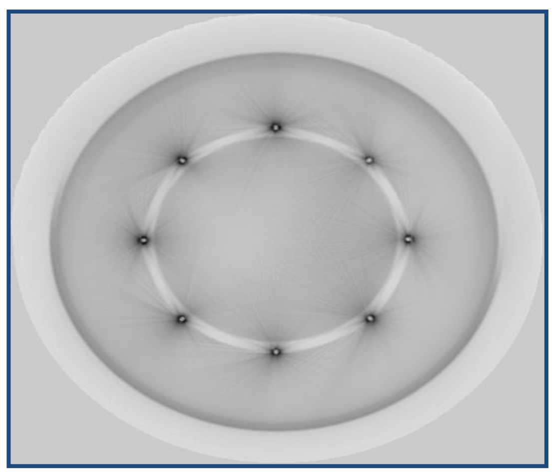

Fig.9b. Phantom down 36.9% from chair
after correction: Slice 64

Conclusion

Following our results, a number of random scans were taken between the midpoint and up position as well as between the mid and down positions using the phantom. Calculating the offsets directly in the c code, the images were successfully reconstructed with high quality without using the geocalibration software. Our experiments showed that indeed the elevator motion was the major cause of the non-isotropic nature of the images. However our random scans did not give images with perfectly uniform beads (Fig.9b) signifying that either the elevator motion is not entirely linear or there may exist other factors other than the elevator causing the non-uniformity.

Acknowledgements

I would like to thank the Fermilab SIST program for offering me the opportunity to take part in this fulfilling research project. Great thanks to my supervisor Thomas Kroc for his wonderful guidance and to Mark Austin (M.A) for his invaluable help, inputs and tutelage.

References

[1] Y Maruyama, J L Beach , J Feola. Scheduling of hypoxic-tumor therapy using neutron brachytherapy. Radiology December 1980 137:775-781.

[2] Brown, Martin J. The Hypoxic Cell: A Target for Selective Cancer Therapy; Eighteenth Bruce F. Cain Memorial Award Lecture. Cancer Res December 1, 1999 *59;* 5863.

[3] Exxim, Software and hardware for x-ray imaging and cone-beam computer tomography. http://www.exxim-cc.com/products_cobra.htm, 2006.

[4] B.J. Mijnheer, J. Rassow, J.R. Williams, J.J. Battermann and A. Wambersie. A neutron-photon treatment planning intercomparison. Radiotherapy and Oncology Volume 3, Issue 2, February 1985, Pages 151-164.

[5] Ugo Amaldi, Cancer therapy with particle accelerators. Nuclear Physics A, Volume 654, Issues 1-2, 26 July 1999, Pages C375-C399.Proceedings of the International Nuclear Physics Conference.

[6] About Fermilab.History, December 20, 2001. http://www.fnal.gov/pub/about/whatis/history.html.

[7] Seattle Cancer Care Alliance, 2004. http://www.seattlecca.org/diseases/salivary-gland-cancer-treatment-neutron-therapy.cfm

[8] Vaupel P, Harrison L. Tumor Hypoxia: Causative Factors, Compensatory Mechanisms, and Cellular Response. The Oncologist 2004; 9 (suppl 5):4-9

[9] Russell KJ, Caplan RJ, Laramore GE, et al. Photon versus fast neutron external beam radiotherapy in the treatment of locally advanced prostate cancer: results of a randomized prospective trial. International Journal of Radiation Oncology, Biology, Physics 28(1): 47-54, 1993.

[10] Anand P. S, Strauss J.B, Kirk M.C. Chen S.S., Kroc T.K, Zusag T.W.Upright 3D Treatment Planning Using a Vertical CT. Medical Dosimetry, Volume 34, Issue 1, Pages 82-86, 2009

[11] Unimeasure HXP510 Series manual, http://www.unimeasure.com/obj--pdf/pdf-hx-p510.pdf